

Potential and current distribution on the surface of a hydrogen gas diffusion anode

J. J. T. T. VERMEIJLEN*, L. J. J. JANSSEN

Eindhoven University of Technology, Department of Chemical Engineering, Laboratory of Instrumental Analysis, PO Box 513, 5600 MB Eindhoven, The Netherlands

A. J. GEURTS

Eindhoven University of Technology, Department of Mathematics and Computing Science, PO Box 513, 5600 MB Eindhoven, The Netherlands

G. C. VAN HAASTRECHT

Hoogovens Group B.V., Department of Packaging Technology, PO Box 10.000, 1970 CA IJmuiden, The Netherlands

Received 23 February 1995; revised 5 May 1995

The current and potential distribution for a hydrogen gas-diffusion disc electrode with a relatively high ohmic resistance are investigated. A theoretical model for these distributions is presented. Potential differences between the edge of the electrode and points on the electrode surface have been measured for a hydrogen gas-diffusion electrode loaded with various total currents. From the results it is concluded that the proposed model is very useful to obtain the potential and the current density distribution along a hydrogen-gas diffusion disc electrode. Moreover, the allowable size of cylindrical holes in a perforated plate placed against the rear of the gas diffusion electrode for its current supply, can be calculated to achieve a reasonably uniform current distribution along the gas-diffusion electrode.

List of symbols

| | |
|---------------|---|
| a | dimensionless radius |
| E_e | equilibrium potential (V) |
| f | constant at constant temperature, $f = \mathcal{F}/RT$ (V^{-1}) |
| \mathcal{F} | Faraday constant ($96\,500\text{ A s mol}^{-1}$) |
| i | current density ($A\text{ m}^{-2}$) |
| i_0 | exchange current density ($A\text{ m}^{-2}$) |
| I | current (A) |
| r | radius (m) |
| r_0 | radius of circular electrode (m) |
| R^{\square} | square resistance (Ω) |
| R | gas constant ($R = 8.314\text{ J K}^{-1}\text{ mol}^{-1}$) |
| t_e | thickness of electrode (m) |

T temperature (K)

Wa Wagner number

Greek letters

| | |
|------------|---|
| γ | electrode efficiency |
| η | overpotential (V) |
| ρ | specific resistance ($\Omega\text{ m}$) |
| ϕ | potential (V) |
| α_v | charge transfer coefficient |

Subscripts

| | |
|-----|-----------------------------------|
| av | average |
| e | electrode, equilibrium conditions |
| max | maximum |
| s | surface |
| tot | total |

1. Introduction

The electrical resistivity of gas diffusion electrodes is relatively high and special attention has to be paid to their method of contact for current supply. To obtain a uniform current distribution along the electrode surface a perforated flat plate or an expanded metal gauze are placed against the rear of the gas diffusion electrode. Many authors have dealt with the secondary current distribution or potential

distribution for resistive electrodes. For such electrodes, only a part of the electrical energy supplied is used for the electrode reactions. The rest is converted into heat within the electrode.

Various aspects of resistive electrodes have been the subject of investigation, e.g. the electrode shape [1–4], the current feeder configuration [5] and the ratio of ohmic and kinetic resistance and the consequences for current distribution [6]. For porous electrodes, the ratio of matrix conductance and ionic conductance

* Present address: ODME, R&D Department, PO Box 832, 5600 AV, Eindhoven, The Netherlands.

[7] and effects of gas depletion [8] on the current distribution have also been investigated.

In this paper, the potential distribution on the surface of a gas diffusion electrode is presented for various current densities. The specific resistance of the electrode is determined. A model is given to describe the current density and potential distribution on the electrode surface.

2. Experimental details

The experimental setup has been described in [9] and is shown in Fig. 1. The gas used was pure hydrogen gas from a cylinder. The solution was 0.5 M H_2SO_4 prepared from 95–97% p.a. sulphuric acid (Merck) and distilled, deionized water.

Hydrogen gas was supplied to the gas side of the gas diffusion electrode at a volumetric flow rate of $5 \text{ cm}^3 \text{ s}^{-1}$. The solution was kept at a constant temperature of 298 K and was recirculated through the solution compartment of the test cell at a volumetric flow rate of $5 \text{ cm}^3 \text{ s}^{-1}$. The gas diffusion electrode used was a 'fuel cell grade electrode' on Toray Paper purchased from E-TEK, USA loaded with $0.5 \text{ mg cm}^{-2} \text{ Pt}$.

Since radial symmetry considerably facilitates calculations, the gas diffusion electrode was mounted in the test cell as shown in Fig. 1. The current was supplied to the gas diffusion electrode through a $20 \mu\text{m}$ platinum sheet pressed against the electrode on the solution side of the electrode. A circular opening with a radius of 1 cm was cut in the platinum sheet. The sheet was pressed against the electrode by a Perspex plate with an identical circular opening. An identical platinum sheet was pressed against the gas side of the electrode by a perforated Perspex support. On the perforated Perspex support, small electrical contacts were mounted. These contacts were pressed against the gas diffusion electrode to facilitate

potential difference measurements at the gas side of the electrode. The insulated wires connected to these contacts left the gas chamber of the cell through the gas outlet.

Currents were supplied to the cell from a Delta Elektronika SM 6020 power supply. Potentials were measured with a Keithley 177 microvolt digital multimeter. The specific resistance of the gas diffusion electrode was measured using a four point probe built in-house [10].

3. Results

The specific resistance of the electrode, ρ_e , as calculated from four point probe measurements, was $(1.40 \pm 0.2) \times 10^{-4} \Omega \text{ m}$. The average electrode thickness was $(5.2 \pm 0.2) \times 10^{-4} \text{ m}$.

Figure 2 shows typical results from measurements of the electrode potential difference between the current supply of the working electrode at the liquid side of the electrode and the measurement points at the gas side of the electrode. The reproducibility of the measurements was extremely high. The edge of the electrode corresponds to the measuring point at $r = 10^{-2} \text{ m}$, being the edge of the open disc of the platinum sheets at the gas side and the liquid side of the electrode, and the centre of the electrode corresponds to $r = 0 \text{ m}$.

Figure 2 shows a significant potential difference between the liquid side edge and the gas side edge of the electrode. This potential difference increases linearly with increasing current and is attributed to the contact resistance between the platinum sheet at the liquid side and the gas diffusion electrode, which amounts to 0.011Ω . Measurements were corrected for the potential loss due to this contact resistance to obtain the corrected potential difference, $\Delta\phi_e$, due to the ohmic resistance of the gas diffusion electrode. The corrected results are shown in Fig. 3.

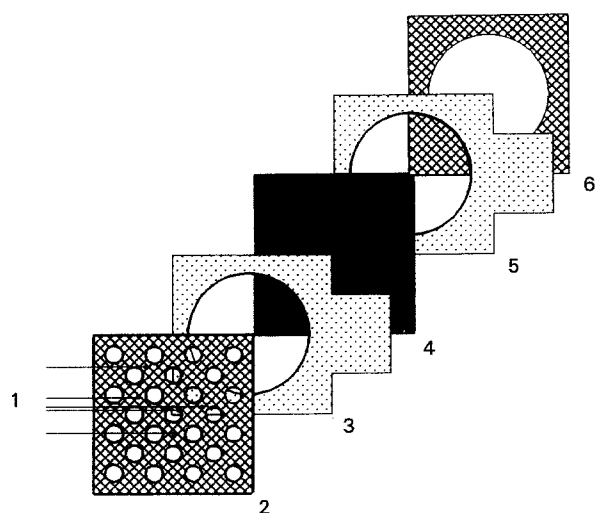


Fig. 1. Exploded view of the gas diffusion electrode assembly for potential difference measurements. (1) Contact wires, (2) perforated Perspex support with electrical contacts, (3) platinum contact sheet, (4) gas diffusion electrode, (5) platinum sheet, working electrode connection to power supply, (6) Perspex support.

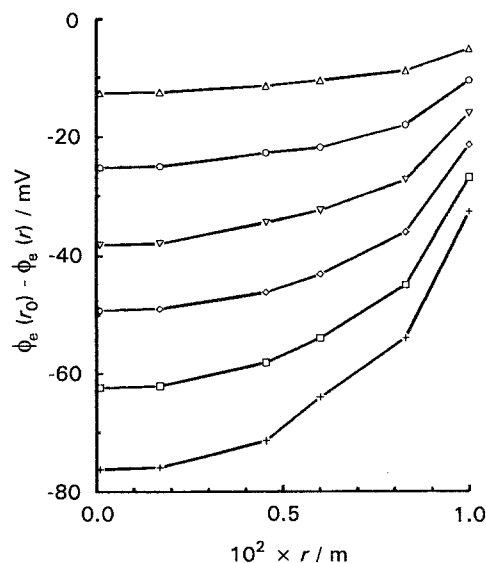


Fig. 2. Potential differences measured between the working electrode connection at the liquid side of the gas diffusion electrode and the contacts at the gas side of the electrode for a total current, I_{tot} : (Δ) 0.5, (\circ) 1.0, (∇) 1.5, (\diamond) 2.0, (\square) 2.5 and ($+$) 3.0 A.

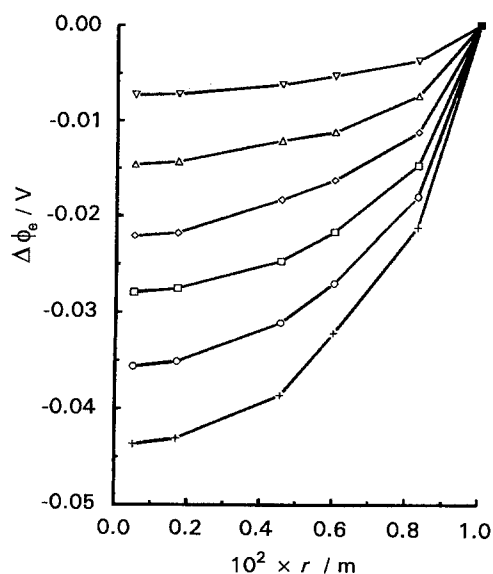


Fig. 3. The data from Fig. 2, corrected for the potential drop due to the contact resistance. I_{tot} : (∇) 0.5, (Δ) 1.0, (\diamond) 1.5, (\square) 2.0, (\circ) 2.5 and ($+$) 3.0 A.

Attempts to determine accurately the potential drop between the working electrode and the tip of the Luggin capillary, using the current interruption method, failed because of the inaccuracy of such measurements.

4. Theory

In this Section, an equation is derived to estimate the theoretical potential drops over the surface of a resistive electrode. The theoretical framework is based on previous work [11]. The gas diffusion electrodes consists of two layers, viz. the active (hydrophilic) layer of approximately 0.1 mm thickness, and the inactive (hydrophobic) layer of approximately 0.45 mm thickness. Because of a large difference in layer thickness the gas diffusion electrode is considered a one-layer electrode.

A disc electrode with thickness t_e and radius r_0 , as shown in Fig. 4, is discussed. If $t_e \ll r_0$, potential drops in the axial direction of the cylinder can be neglected. The specific resistance of the electrode material is ρ_e .

The circular electrode can be considered as divided into concentric rings with width Δr . Figure 5 shows part of a ring of the electrode.

The current I_e entering the ring at radius r can be described by

$$I_e(r) = 2\pi r t_e i_e(r) \quad (1)$$

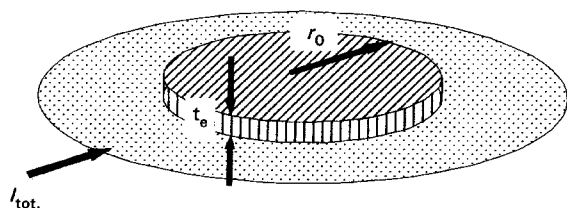


Fig. 4. Schematic representation of a circular electrode with peripheral current collector. Electrode radius r_0 , electrode thickness t_e .

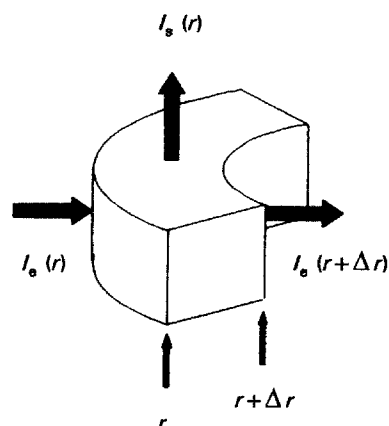


Fig. 5. Segment of a ring of a circular electrode with currents entering and leaving the ring indicated.

The current from the electrode into the solution, I_s , due to the electrochemical reaction at the ring with a surface area of $2\pi r \Delta r$ can be described by

$$I_s(r) = 2\pi r \Delta r i_s(\eta(r)) \quad (2)$$

where $i_s(\eta(r))$ is the reaction current density, which is a function of the electrode overpotential. The current balance for a ring can be written as

$$I_e(r + \Delta r) - I_e(r) = I_s(r) \quad (3)$$

Using Equations 2 and 3 and taking $\Delta r \rightarrow 0$, it follows that

$$\frac{dI_e(r)}{dr} = 2\pi r i_s(\eta(r)) \quad (4)$$

For the electrode material, Ohm's law applies. The change in electrode potential is given by

$$\frac{d\phi_e(r)}{dr} = -\rho_e i_e(r) \quad (5)$$

Differentiation of Equation 1 with respect to r gives

$$\frac{dI_e(r)}{dr} = 2\pi t_e i_e(r) + 2\pi r t_e \frac{di_e(r)}{dr} \quad (6)$$

Differentiation of Equation 5 gives

$$\frac{d^2\phi_e(r)}{dr^2} = -\rho_e \frac{di_e(r)}{dr} \quad (7)$$

Combination of Equations 4–7 gives

$$\frac{d^2\phi_e(r)}{dr^2} + \frac{1}{r} \frac{d\phi_e(r)}{dr} + \frac{\rho_e}{t_e} i_s(\eta(r)) = 0 \quad (8)$$

The overpotential η is given by

$$\eta(r) = \phi_e(r) - \phi_s(r) - E_e(r) \quad (9)$$

according to [3]. If the electrolyte is considered radially equipotential ($d\phi_s(r)/dr = 0$) and if E_e for the electrochemical reaction does not change with r ($dE_e(r)/dr = 0$), Equation 9 can be differentiated to give

$$\frac{d\eta(r)}{dr} = \frac{d\phi_e(r)}{dr} \quad (10)$$

implying the change in electrode overpotential, η , is equal to the change in electrode potential, ϕ_e . Combination of Equations 8 and 10 yields the differential

equation to be solved:

$$\frac{d^2\eta(r)}{dr^2} + \frac{1}{r} \frac{d\eta(r)}{dr} + \frac{\rho_e}{t_e} i_s(\eta(r)) = 0 \quad (11)$$

The Butler–Volmer equation for i_s as a function of η is

$$i_s(\eta(r)) = i_0[\exp(\alpha_V f \eta(r)) - \exp(-(1 - \alpha_V) f \eta(r))] \quad (12)$$

where $f = \mathcal{F}/RT$.

Equation 12 has been used successfully to describe the current–potential curve up to 3 kA m^{-2} for hydrogen oxidation on a fully active gas diffusion electrode under pure hydrogen-gas conditions [12].

The dimensionless radius is defined as

$$a = r/r_0 \quad (13)$$

To describe the current distribution the Wagner number is used [13]. This represents the ratio of the polarization resistance and the electrode resistance and is defined as

$$Wa = (i_0 R^\square r_0^2 f)^{-1} \quad (14)$$

where R^\square is the square resistance of the electrode material [10], defined by

$$R^\square = \rho_e/t_e \quad (15)$$

Equation 11 can be rewritten using Equations 12–15 to give

$$\frac{d^2\eta(a)}{da^2} + \frac{1}{a} \frac{d\eta(a)}{da} + (f Wa)^{-1} [\exp(\alpha_V f \eta(a)) - \exp((\alpha_V - 1) f \eta(a))] = 0 \quad (16)$$

Boundary conditions for Equation 16 are as follows:

$$\left(\frac{d\eta(a)}{da} \right)_{a=0} = 0 \quad \text{at} \quad a = 0$$

and

$$\eta(a) = \eta(1) \quad \text{at} \quad a = 1$$

where $\eta(1)$ is a known or assumed quantity and $\eta(a)$ is the electrode overpotential at the edge of the electrode.

The electrode efficiency, γ , is defined as the quotient of the average current density, i_{av} , and the maximal current density, i_{max} . From Equations 1, 5, 10, 13 and 15 the total current into the electrode is described by

$$I_{tot} = \frac{-2\pi}{R^\square} \left(\frac{d\eta(a)}{da} \right)_{a=1} \quad (17)$$

The average current density is therefore given by

$$i_{av} = \frac{I_{tot}}{\pi r_0^2} = \frac{-2}{R^\square r_0^2} \left(\frac{d\eta(a)}{da} \right)_{a=1} \quad (18)$$

The maximal current density is given by the current density, i_s , at $r = r_0$. From Equations 12, 14 and 18 it is found that

$$\gamma = \frac{i_{av}}{i_{max}} = -2 \frac{f Wa \left(\frac{d\eta(a)}{da} \right)_{a=1}}{\exp(\alpha_V f \eta(1)) - \exp((\alpha_V - 1) f \eta(1))} \quad (19)$$

Equation 16 was solved numerically for various values of Wa and η with $\alpha_V = 0.5$ and $f = 38.95 \text{ V}^{-1}$ using a Fortran program with the D02HAF routine from the NAG library. The electrode efficiency was calculated using Equation 19 with the results of the numerical solutions of Equation 16.

In Fig. 6, the effect of Wa on the relation between the electrode overpotential at the edge of the electrode and the average reduced current density on the electrode surface is illustrated. In Fig. 7, the effect of Wa on the relation between the electrode overpotential difference between the edge and the centre of the electrode and the average reduced current density is shown. In Fig. 8, the effect of Wa on the relation between the electrode efficiency and the average reduced current density is shown.

If for a specific electrode and a specific electrochemical reaction the radius r_0 , the thickness t_e , the specific resistance ρ_e and the exchange current density i_0 are known, Fig. 8 can be used to determine the electrode efficiency at the required average current density. Figure 7 can be used to estimate the overpotential drop in the electrode under these circumstances and the electrode edge potential can be read from Fig. 6. The difference between the edge and the centre potential is a measure of the potential difference across the electrode surface. The maximum current density, i_{max} , is equal to the average current density, i_{av} , divided by the efficiency, γ , according to Equation 19. The minimal current density is calculated from Equation 12 where the overpotential is the overpotential in the centre of the electrode. The difference between minimal and maximal current density is a measure of the current distribution across the electrode surface.

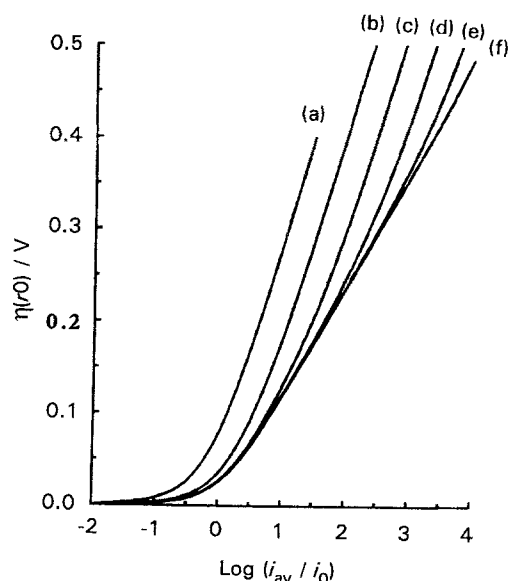


Fig. 6. The overpotential at the edge of the electrode, $\eta(r_0)$, is plotted against the average reduced current density, i_{av}/i_0 for $\alpha_V = 0.5$, $T = 298 \text{ K}$ ($f = 38.95 \text{ V}^{-1}$) and for Wa : (a) 2.57×10^{-2} , (b) 2.57×10^{-1} , (c) 2.57 , (d) 2.57×10^1 , (e) 2.57×10^2 and (f) 2.57×10^3 .

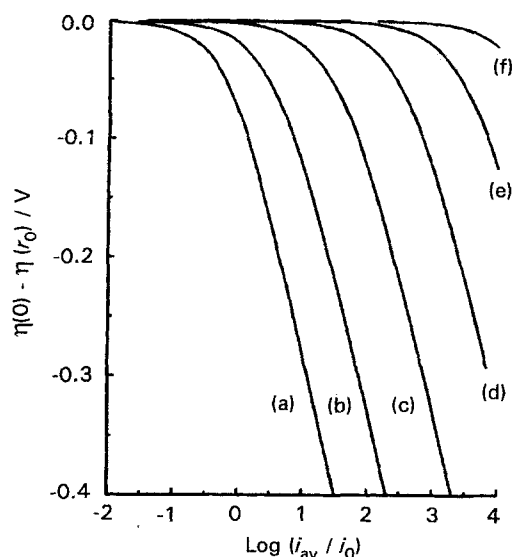


Fig. 7. The potential difference between the centre and the edge of the electrode, $\eta(0) - \eta(r_0)$, as a function of the average reduced current density, i_{av}/i_0 for $\alpha_v = 0.5$, $T = 298$ K ($f = 38.95$ V $^{-1}$) and for Wa : (a) 2.57×10^{-2} , (b) 2.57×10^{-1} , (c) 2.57, (d) 2.57×10^1 , (e) 2.57×10^2 and (f) 2.57×10^3 .

5. Discussion

The specific resistance of the electrode can be determined from results as presented in Fig. 3. From Equation 17 it can be shown that

$$\rho_e = \frac{2\pi r_0 t_e}{I_{tot}} \left(\frac{d\phi_e(r)}{dr} \right)_{r=r_0} \quad (20)$$

where I_{tot} is the total current flowing into the electrode from the power source. Applying Equation 20 to the measured potential differences near the edge of the electrode, a value for ρ_e of $(1.30 \pm 0.05) \times 10^{-4}$ Ω m was calculated. This measurement is inaccurate due to the large change in the slope in the range from $r = 0.8$ to 1.0 cm. The value is, however, in good

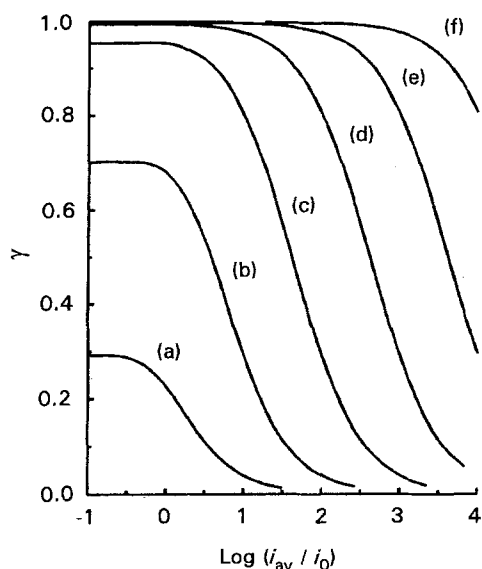


Fig. 8. The electrode efficiency, γ , as a function of the average reduced current density, i_{av}/i_0 for $\alpha_v = 0.5$, $T = 298$ K ($f = 38.95$ V $^{-1}$) and for Wa : (a) 2.57×10^{-2} , (b) 2.57×10^{-1} , (c) 2.57, (d) 2.57×10^1 , (e) 2.57×10^2 and (f) 2.57×10^3 .

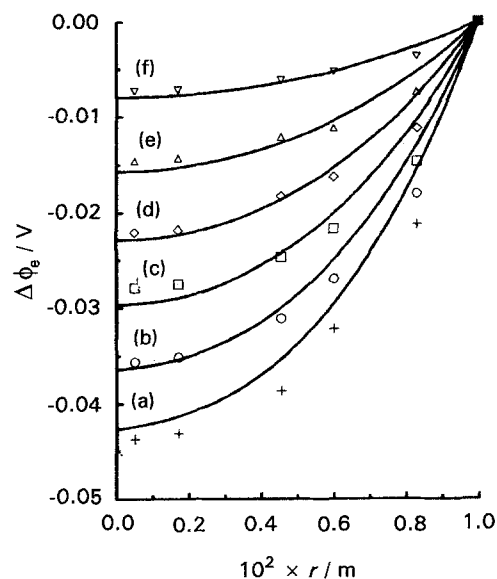


Fig. 9. The calculated and the measured potential differences between the edge of the electrode and a point on the electrode surface, $\Delta\phi_e$, as a function of the radius. $r_0 = 10^{-2}$ m, $i_0 = 1.2$ kA m $^{-2}$, $R^{\square} = 0.22$ Ω . The total current, I_{tot} : (+, a) 3.0, (O, b) 2.5, (\square , c) 2.0, (\diamond , d) 1.5, (Δ , e) 1.0 and (∇ , f) 0.5 A.

agreement with the directly determined value of $(1.40 \pm 0.2) \times 10^{-4}$ Ω m from Section 3. Using $\rho_e = 1.30 \times 10^{-4}$ Ω m and $t_e = 5.2 \times 10^{-4}$ m from Section 3, a value of 0.25 Ω was calculated for R^{\square} . In [9] a value of 760 A m $^{-2}$ was calculated for the exchange current density, i_0 . Since $r_0 = 10^{-2}$ m, an estimated value for Wa of 1.35 is obtained.

By trial and error and using $Wa = 1.35$ as a starting value, it was found that a good approximation for the data from Fig. 3 can be obtained with $r_0 = 10^{-2}$ m, $R^{\square} = 0.22$ Ω and $i_0 = 1200$ A m $^{-2}$. The value for R^{\square} is in good agreement with that obtained above and the value of i_0 with that obtained from polarization curves [12]. Using the resulting value, $Wa = 0.97$, the potential difference between the edge of the

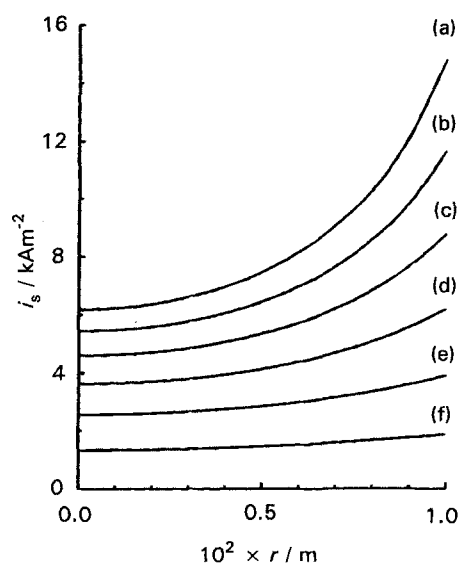


Fig. 10. The current density on the electrode surface, i_s , as a function of the place on the electrode, r , as calculated from Equation 16 for $r_0 = 10^{-2}$ m, $i_0 = 1.2$ kA m $^{-2}$, $R^{\square} = 0.22$ Ω . The total current, I_{tot} : (a) 3.0, (b) 2.5, (c) 2.0, (d) 1.5, (e) 1.0 and (f) 0.5 A.

electrode and various points on the electrode, $\Delta\phi_e$, for the total currents from Fig. 3 were calculated using Equations 16 and 18. The calculation procedure was based on a Fortran program with the DO2HAF routine from the NAG library. The results are shown in Fig. 9. The agreement between the calculated and measured potential differences is good.

Figure 10 shows the current density distribution at various total currents where overpotential distribution from Fig. 9 has been used. It can be seen that the current density distribution becomes more unequal with increasing current, in particular at currents higher than approximately 1 A. The calculated electrode efficiencies range from 0.65 at a total current of 3 A to 0.85 at a total current of 0.5 A. Calculations show that, to increase the electrode efficiency from 0.65 to ~ 0.9 at an average current density of 9.5 kA m^{-2} , the electrode radius has to decrease from 10 to 4.3 mm.

It can be concluded that the ohmic resistance of the gas diffusion electrode may play a major role in both current and overpotential distribution. The expressions derived can be used to calculate the current density distribution and electrode efficiency. The results also emphasize the importance of a sufficient

number of uniformly distributed contact points between the gas diffusion electrode and the current collector (e.g., metal gauze or expanded metal) placed against the back side of the gas diffusion electrode to ensure both good current distribution and electrode efficiency.

References

- [1] P. M. Robertson, *Electrochim. Acta* **22** (1972) 411.
- [2] K. Scott, *J. Appl. Electrochem.* **13** (1983) 209.
- [3] J. M. Bisang and G. Kreysa, *ibid.* **18** (1988) 422.
- [4] A. J. Grabowsky and J. Newman, *J. Electrochem. Soc.* **140** (1993) 1625.
- [5] Y. Nishiki, K. Aoki, K. Tokuda and H. Matsuda, *J. Appl. Electrochem.* **17** (1987) 445.
- [6] A. C. West and J. Newman, *J. Electrochem. Soc.* **136** (1989) 2935.
- [7] S. L. Marshall, in *Proceedings of the Symposia on Electrochemical Engineering and Small Scale Electrolytic Processing*. Proceedings of the Electrochemical Society, (The Electrochemical Society, Pennington, NJ) vol. 90 (1990) p. 189.
- [8] R. P. Iczkowski and M. B. Cutlip, *J. Electrochem. Soc.* **127** (1980) 1433.
- [9] J. J. T. T. Vermeijlen and L. J. J. Janssen, *J. Appl. Electrochem.* **23** (1993) 26.
- [10] P. J. Severin, *Philips Research Reports* **26** (1971) 279.
- [11] J. H. Naus, unpublished, (1983).
- [12] J. J. T. T. Vermeijlen, PhD thesis, Eindhoven (1994).
- [13] C. Wagner, *J. Electrochem. Soc.* **98** (1951) 116.